PCCP

RSC Publishing

PAPER

View Article Online
View Journal | View Issue

Cite this: *Phys. Chem. Chem. Phys.*, 2013, **15**, 13147

First spectroscopic identification of pyrocarbonate for high CO_2 flux membranes containing highly interconnected three dimensional ionic channels

Lingling Zhang,[a] Xinyu Huang,[a] Changyong Qin,[b] Kyle Brinkman,[c] Yunhui Gong,[a] Siwei Wang[a] and Kevin Huang*[a]

Received 6th June 2013,
Accepted 6th June 2013

DOI: 10.1039/c3cp52362d

www.rsc.org/pccp

Identification of the existence of pyrocarbonate ion $C_2O_5^{2-}$ in molten carbonates exposed to a CO_2 atmosphere provides key support for a newly established bi-ionic transport model that explains the mechanisms of high CO_2 permeation flux observed in mixed oxide-ion and carbonate-ion conducting (MOCC) membranes containing highly interconnected three dimensional ionic channels. Here we report the first Raman spectroscopic evidence of $C_2O_5^{2-}$ as an active species involved in the CO_2-transport process of MOCC membranes exposed to a CO_2 atmosphere. The two new broad peaks centered at 1317 cm^{-1} and 1582 cm^{-1} are identified as the characteristic frequencies of the $C_2O_5^{2-}$ species. The measured characteristic Raman frequencies of $C_2O_5^{2-}$ are in excellent agreement with the DFT-model consisting of six overlapping individual theoretical bands calculated from $Li_2C_2O_5$ and $Na_2C_2O_5$.

Introduction

Manmade CO_2 emission through the use of fossil fuels is thought to be a major source for global warming and climate change. The stabilization of atmospheric CO_2 concentration is generally considered as the best near-term solution to mitigate the negative environmental impacts caused by burning fossil fuels. The current mainstream technical approach to achieving that goal is to curb the emission of CO_2 by capturing CO_2 at point-sources and geologically storing it. So far, three industrial combustion processes have been identified as the point-sources for carbon removal:[1–10] pre-combustion, post-combustion and oxy-combustion. Significant technical progress in materials development and engineering design of carbon capture systems has been made over the past few decades, but the major challenge to the commercial deployment of these technologies remains to be the energy penalty associated with CO_2 capture, compression and storage (CCS) that considerably lowers the overall plant efficiency and ultimately increases the cost-of-electricity produced.

The state-of-the-art technologies for CO_2-capture are principally based on reversible chemical–physical sorption processes using liquid solvents and solid sorbents as CO_2 scrubbers[11–13] and on size-exclusion permeation using membranes as CO_2 molecular filters.[14–19] However, as aforementioned, the solvents and sorbents based technology is cost prohibitive and energy intensive,[20–24] and the membrane technology is susceptible to poor selectivity and incompatibility at high temperatures.[25–28] As of today, only a few of these technologies are considered commercially ready for large-scale application.

In an effort to advance the CCS technology, we as well as other research groups have recently studied a new type of electrochemical CO_2 separation membranes that are in theory exclusively permeable to CO_2 and compatible with elevated temperatures.[5,29–33] The new electrochemical membranes consist of an oxide-ion conducting porous matrix densely filled with a carbonate-ion conducting alkali carbonate melt, which constitutes a dual-phase mixed oxide-ion and carbonate-ion conductor (MOCC). CO_2 is transported through the membrane in the form of CO_3^{2-}, which is charge-compensated by a concomitant flow of O^{2-}. Therefore, the MOCC membranes are more suited for pre-combustion application where the feedstock gas is a mixture of CO_2 and H_2. We have particularly shown that the solid oxide-ion conductor of the porous matrix synthesized using a combined ''co-precipitation'' and ''sacrificial-template'' method encompasses abundant highly-interconnected ionic channels with well-defined and tunable microstructural features for fast CO_2 transport.[5,34,35] The CO_2 permeation flux density measured from these membranes exposed to CO_2–H_2

[a] *Department of Mechanical Engineering, University of South Carolina, Columbia, SC 29201, USA. E-mail: kevin.huang@sc.edu*
[b] *Department of Biology, Chemistry and Environmental Health Science, Benedict College, Columbia, South Carolina 29204, USA*
[c] *Materials Science & Technology, Savannah River National Laboratory, Aiken, SC 29808, USA*

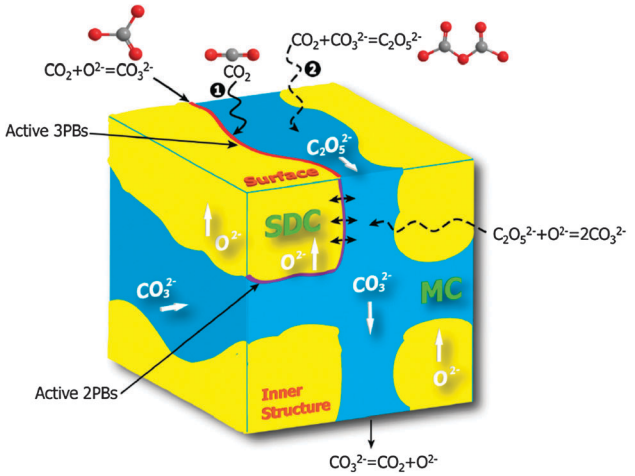

Fig. 1 A 3D-schematic illustrating electrochemical reaction occurring at 3PBs to 2PBs in dual-phase MOCC membranes; SDC = Sm_2O_3-doped CeO_2; MC = molten carbonate.

feed gas is remarkable, attaining $J_{CO_2} \geq 1$ mL min^{-1} cm^{-2} and averaging nearly two orders of magnitude higher than membranes developed by other groups.[30,31]

To understand the fundamentals of a high-flux CO_2 transport phenomenon through the MOCC membranes, we propose for the first time a multi-pathway bi-ionic transport model schematically shown in Fig. 1. The core of the new model is an ionic pathway (denoted as Pathway-2) along the two-phase boundaries (2PBs) between solid-oxide and molten-carbonate (MC), which is parallel to the ionic pathway at the three-phase-boundaries (3PBs) (denoted as Pathway-1). The Pathway-1 is a conventional route that considers surface ionization of CO_2 solely at 3PBs, where CO_2, O^{2-} and CO_3^{2-} are simultaneously available at the feed surface, and subsequent transport of CO_3^{2-} through the MC phase and deionization of CO_3^{2-} on the permeate surface.

$$CO_{2(g)} + O_{(SO)}^{2-} \underset{\text{permeate}}{\overset{\text{feed}}{\rightleftharpoons}} CO_{3(MC)}^{2-} \quad (1)$$

Here the subscripts (g), (SO) and (MC) represent gas, solid-oxide and molten carbonate phases, respectively. During the CO_2 transport, the flux of CO_3^{2-} is charge-compensated by the flow of O^{2-}. The theoretical CO_2 flux density J_{CO_2} through 3PBs can be calculated by[5]

$$J_{CO_2} = -\left(\frac{\varepsilon}{\tau}\right)\frac{RT}{4F^2L}\frac{\varphi\sigma_c(1-\varphi)\sigma_o}{\varphi\sigma_c + (1-\varphi)\sigma_o}\ln\frac{P''_{CO_2}}{P'_{CO_2}} \quad (2)$$

Here ε and τ are the porosity and tortuosity of the porous oxide matrix, respectively; σ_c and σ_o are ionic conductivities of the carbonate ion and the oxide ion, respectively; P'_{CO_2} and P''_{CO_2} are the partial pressure of CO_2 at the feed and permeate sides, respectively; φ is the volumetric fraction of the MC phase; L is the thickness of the membrane, and R, T and F have their usual meanings. The CO_2 ionization reaction (1) has been widely suggested in the literature as the global mechanism for CO_2 transport in dual-phase MOCC, but proceeding at a relatively slow rate.[36–38]

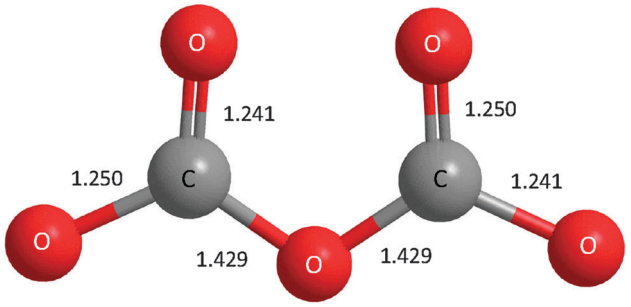

Fig. 2 Equilibrium geometry of the $C_2O_5^{2-}$ species. The unit of bond length is in Å.

The Pathway-2 encompasses surface ionization of CO_2 at 2PBs of the CO_2/MC interface and internal ionic transfer at 2PBs of the SDC/MC interface. The species $C_2O_5^{2-}$ (pyrocarbonate or dicarbonate anion) possessing a $(CO_2)_n$ chainlike structure as shown in Fig. 2 is deemed an intermediate product of CO_2 chemisorption on the surface of MC *via*

$$CO_{2(g),feed} + CO_{3(MC)}^{2-} = C_2O_{5(MC)}^{2-} \quad (3)$$

Once formed, $C_2O_5^{2-}$ can immediately react with O^{2-} available at the SDC/MC interface, dissociating into two CO_3^{2-} that can migrate to 3PBs on the permeate surface, where much faster CO_3^{2-} deionization reaction takes place to release CO_2 and O^{2-}.

$$C_2O_{5(MC)}^{2-} + O_{(SO)}^{2-} = 2CO_{3(MC)}^{2-} \quad (4)$$

$$CO_{3(MC)}^{2-} = CO_{2(g),permeate} + O_{(SO)}^{2-} \quad (5)$$

The overall reaction of the CO_2-transport is, therefore, given by

$$CO_{2(g),feed} = CO_{2(g),permeate} \quad (6)$$

Overall, the reactive zones for the CO_2-transport are extended from 3PBs to 2PBs, significantly increasing the reactive areas, thus being largely responsible for the observed high CO_2 flux. Key support to the above new bi-ionic transport model is the experimental evidence of $C_2O_5^{2-}$ existing on the surface of a MC exposed to a CO_2 atmosphere. The likelihood of absorbing CO_2 on the surface of a MC to form $C_2O_5^{2-}$ has been suggested by Claes *et al.*[36–38] who studied the solubility and solvation of CO_2 in a molten eutectic mixture of Li_2CO_3–Na_2CO_3–K_2CO_3 at 973 K. They found CO_2 to be extremely soluble in MC. The measured 0.1 mol per liter per atm solubility is well beyond what is expected from Henry's law. The authors concluded that chemical absorption was taking place, most probably by the reaction of $CO_{3(MC)}^{2-} + CO_{2(g)} = C_2O_{5(MC)}^{2-}$. DFT calculations were carried out by the authors to gain insight into the reaction energetics. The calculated values for ΔH^0 and ΔG^0 are −223 kJ mol^{-1} and −119 kJ mol^{-1} at 973K, respectively, indicating favorable gas-phase energetics, and solvation should not hinder the formation of the postulated $C_2O_5^{2-}$ in the MC. Furthermore, another study reported cross-over ^{13}C-NMR experiments between [^{13}C] and [^{18}O] carbonates

in aqueous solutions of Na_2CO_3.[39] The complex kinetic problem was interpreted as giving evidence for the existence of the $CO_3^{2-}{}_{(aq)}$+ $CO_{2(g)}$ = $C_2O_5^{2-}{}_{(aq)}$ equilibrium under these experimental conditions. Based on these early studies, it is, therefore, conceivable that the formation of $C_2O_5^{2-}$ species in MC by chemical absorption of CO_2 could well be a facile process. However, so far no direct experimental observation of the existence of $C_2O_5^{2-}$ species in MC has been reported.

Here we report for the first time spectroscopic observation of the $C_2O_5^{2-}$ species in a Li_2CO_3–Na_2CO_3 melt surrounded by a CO_2 atmosphere. A standard procedure to identify newly synthesized compounds or species in the chemical world is to record IR and Raman vibrational spectra. This procedure is relevant as long as the vibrational spectrum is not too congested (which usually happens below 900 cm^{-1} because of the superposition of bending, rocking, and torsional modes). *In situ* Raman spectroscopy is, therefore, chosen as the method of study to probe $C_2O_5^{2-}$ species.

Experimental procedures

In situ Raman spectroscopic study

The Li_2CO_3 and Na_2CO_3 eutectic mixture (52 : 48 in mol%) was first synthesized in air at 650 °C. After a 2 h hold, the melt was then quenched to room temperature, followed by breaking into fine particles by ball milling. Thus prepared powders were then packed into a gold crucible that was subsequently loaded into a high temperature stage (Linkam TS1500, 0–1500 °C). The temperature and gas were controlled using a system controller (Linkam PE95). The Raman spectra were recorded using a LabRam/HR confocal Raman system (LabRam Invers, Horiba Jobin-Yvon) with a He–Ne laser operated at 632.8 nm. Since the position of the thermocouple in the high temperature stage is located outside the crucible, the actual and the controlled temperatures of the MC are different. The melting point of the $(Li/Na)_2CO_3$ at 490 °C was used to calibrate the actual temperature. The scattering Raman spectra were collected *in situ* from the carbonate as a function of temperature (in the range of RT–600 °C) and atmosphere (in N_2, air, CO_2).

DFT modeling

DFT calculations were performed at the B3LYP/6-31G(d)[40–44] level using the Gaussian09[45] suite of quantum programs. The geometry of $Li_2C_2O_5$ and $Na_2C_2O_5$ was optimized first, and the vibrational frequencies were then obtained from analytic second derivatives using a harmonic oscillator model. In addition, Raman intensities were computed by numerical differentiation of dipole derivatives with respect to the electric field.[46]

Results and discussion

Temperature dependence of the Raman spectrum

Fig. 3(a) shows the Raman spectra collected from a eutectic Li_2CO_3–Na_2CO_3 (52 mol% Li_2CO_3–Na_2CO_3) melt over a band range of 650–1850 cm^{-1} as a function of temperature in a pure CO_2 atmosphere. For the carbonate in the solid state, the

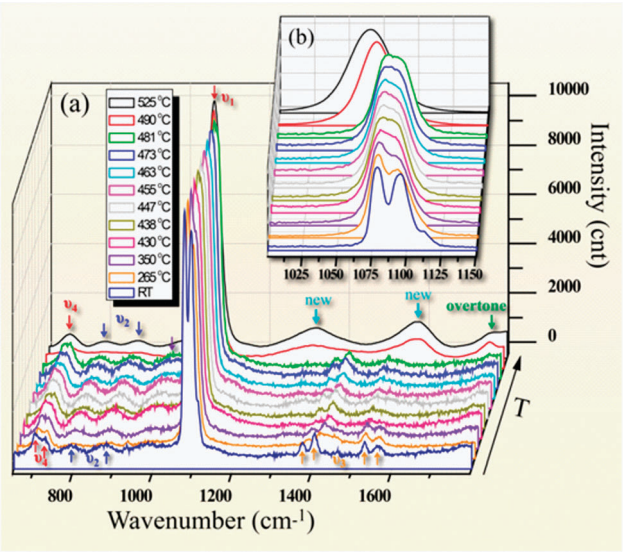

Fig. 3 (a) The Raman spectra of $(Li/Na)_2CO_3$ in the region of 650–1850 cm^{-1} as a function of temperature in a CO_2 atmosphere; (b) magnified view in the region of 1000–1150 cm^{-1}.

Raman spectra are seen to contain four basic vibrational modes relevant to CO_3^{2-} ions. The two bands at 1078 and 1094 cm^{-1} are assigned to ν_1 of symmetric stretching vibrations in Li_2CO_3 and Na_2CO_3, whereas the bands at 792 cm^{-1} and 870 cm^{-1} are assigned to ν_2 of out-of-plane bending vibrations.[47–49] For the isolated CO_3^{2-} that has a D_{3h} symmetry, ν_2 is Raman inactive. However, it is likely that ν_2 becomes Raman active for $(Li/Na)_2CO_3$ due to the distortion of the CO_3^{2-} structure imposed by the cations.[50] The observed bands at 704 and 728 cm^{-1} are assigned to ν_4 of in-plane bending vibrations. This mode is a double degeneration for the distorted CO_3^{2-} induced by Li^+ and Na^+. As the CO_3^{2-} group becomes distorted from its regular planar symmetry, this mode splits into two components.[51] The bands at 1375 cm^{-1}, 1404 cm^{-1}, 1531 cm^{-1} and 1563 cm^{-1} are attributed to a split ν_3 of the asymmetric stretching vibrations caused by the existence of Li^+ and Na^+ around the CO_3^{2-} ions.[50]

The shift of the Raman band with temperature is better viewed in Fig. 3(b), a magnified spectrum showing the region of the major ν_1-bands at 1078 cm^{-1} and 1094 cm^{-1}. As the temperature increases, the ν_1-bands for Li_2CO_3 and Na_2CO_3 shift toward a lower wavenumber and eventually merge into one broad peak at the melting temperature of 490 °C. This shift is a direct result of lowered force-constant, elongated C–O bond length and weakened Li(Na)–C–O bond strength by increasing temperature.[52] When the temperature reaches the melting point, the overtone of the out-of-plane bending mode ($2\nu_2$) appears at 1762 cm^{-1}.[53] It should be noted that a broad but small peak near 970 cm^{-1} only observed in solid-state carbonates appears not to be directly related to CO_3^{2-}, identification of which is not possible for this study. We speculate that the impurities in the sample could be a source for this unknown peak. A detailed assignment of the measured Raman bands at different temperatures and atmospheres is summarized in Table 1.

Table 1 The Raman frequencies measured and assigned for the eutectic $(Li/Na)_2CO_3$ at selected temperatures and atmospheres

Atmospheres	CO_2				Air	N_2
Temperatures (°C)	RT	350	455	490 (melted)	490 (melted)	490 (melted)
Frequencies (cm^{-1})	704	706	706	707	707	707
ν_4 (weak)	728	720	715	—	—	—
	792	790	789	790	790	790
ν_2 (weak)	879	879	881	882	885	885
	1078	1077	1077	1070	1072	1072
ν_1 (strong)	1094	1090	1087	—	—	—
	1375	1385	1386	—	1391	1392
	1404	1415	1416	—	1421	1421
ν_3 (weak)	1531	1520	1520	—	—	—
	1563	1555	1545	—	—	—
New peaks (broad)	—	—	—	1317	—	—
				1582		
Overtone ($2\nu_2$)	—	—	—	1762	1762	1762
Unknown	—	—	972	—	—	—

The most distinguishable features of Raman spectra in Fig. 3 are observed when the carbonate is in a molten state. The four bands corresponding to the ν_3 mode disappear from the spectrum while two new broad bands at 1317 cm^{-1} and 1582 cm^{-1} emerge within the same band width. A natural question to ask is: are these newly emerged Raman bands associated with the $C_2O_5^{2-}$ species?

Atmosphere-dependence of the Raman spectrum

To answer this question, we first measured Raman spectra in different atmospheres. According to the enabling electrochemical reaction shown in reaction (3), the formation of $C_2O_5^{2-}$ requires a source of CO_2. Fig. 4 compares the Raman spectra measured in N_2, air and pure CO_2 atmospheres at 490 °C where the carbonate is in a molten state. The bands at 1072 cm^{-1}, 790 cm^{-1} and 885 cm^{-1}, 707 cm^{-1}, 1391 cm^{-1} and 1421 cm^{-1}, 1762 cm^{-1} shown in Fig. 4(a) recorded in a N_2 atmosphere correspond to the symmetric stretching (ν_1), out-of-plane bending (ν_2), in-plane bending (ν_4), asymmetric stretching (ν_3), and the overtone of the out-of-plane bending mode ($2\nu_2$) vibrations, respectively. The Raman spectrum in air is almost identical to that collected in N_2. However, the peaks at 1317 cm^{-1} and 1582 cm^{-1} shown in Fig. 3(c) are only observable in the CO_2 atmosphere. The strong CO_2-dependence of the bands at 1317 cm^{-1} and 1582 cm^{-1} provides a crucial hint to the formation of $C_2O_5^{2-}$ *via* the CO_2 chemisorption reaction of eqn (3).

The theoretical support to the formation of $C_2O_5^{2-}$ is provided by the DFT calculations. The calculations indicate that high Raman activities of $C_2O_5^{2-}$ are within a band width of 1200–1600 cm^{-1}. Specifically, the active Raman bands are predicted at 1366 cm^{-1}, 1531 cm^{-1} and 1566 cm^{-1} for $Li_2C_2O_5$ and 1345 cm^{-1}, 1547 cm^{-1} and 1579 cm^{-1} for $Na_2C_2O_5$, respectively. The recorded spectrum in the band width of 1200–1650 cm^{-1} from the MC within 490–525 °C in a CO_2 atmosphere could, therefore, be an overlap of these characteristic Raman peaks of $Li_2C_2O_5$ and $Na_2C_2O_5$ in this band region. To deconvolute the two unique broad peaks at around 1317 cm^{-1} and 1582 cm^{-1}, we used Guassian–Lorentizian function with the six theoretical Raman frequencies as the standards. The results are shown in Fig. 5, where the black and red lines represent the measured and modeled spectra, respectively. Also shown is the individual spectrum calculated for the pure $Li_2C_2O_5$ and $Na_2C_2O_5$, represented by pink and blue lines, respectively. It appears that the modeled spectrum is dominated by the Na_2CO_3; only one peak at 1566 cm^{-1} is visible for the Li_2CO_3 while the other two are too weak to be seen. This is primarily due to the differences in size and polarizability of the Na^+ and Li^+ ions. Overall, the measured Raman spectrum is in excellent agreement with the DFT calculations if the temperature effect is factored in. To further experimentally verify the $C_2O_5^{2-}$-centered Pathway-2 mechanism, we will measure in a future study the CO_2 permeation flux through a permeation cell with the feed-side surface covered by a layer of MC, where only 2PBs are available for the Pathway-2 mechanism.

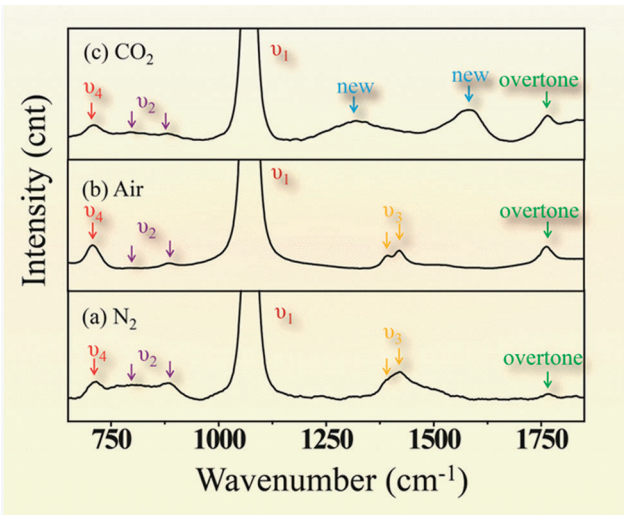

Fig. 4 Raman spectra of the molten $(Li/Na)_2CO_3$ measured as a function of atmosphere at 525 °C.

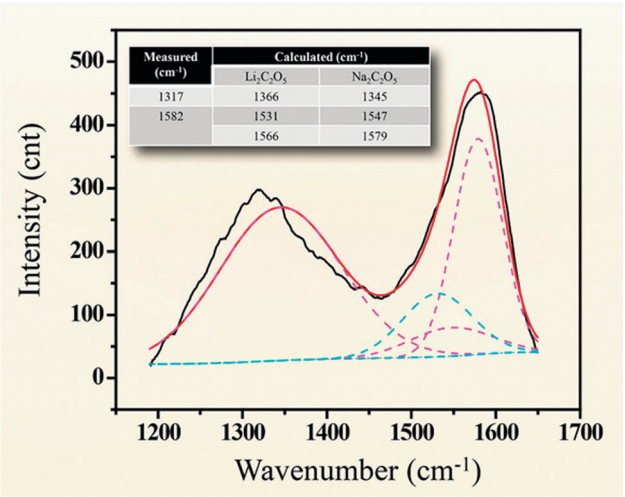

Fig. 5 Deconvolution of the two broad bands observed at 1317 cm^{-1} and 1582 cm^{-1}; inset: the measured and DFT-modeled Raman spectra in a band width of 1200–1650 cm^{-1}.

Conclusion

In summary, we demonstrate the first experimental evidence for the existence of pyrocarbonate $C_2O_5^{2-}$ species in a eutectic Li_2CO_3–Na_2CO_3 melt exposed to a CO_2 atmosphere through a combined ''DFT modeling'' and ''Raman spectroscopy'' approach. The existence of $C_2O_5^{2-}$ species is key support to a new bi-ionic transport model established to elucidate the fundamentals of the high-flux CO_2 transport phenomenon observed in the superior mixed oxide-ion and carbonate-ion conducting CO_2 separation membranes. The broad Raman bands centered at 1317 cm^{-1} and 1582 cm^{-1} are characteristic of $C_2O_5^{2-}$ species in molten carbonates exposed to a CO_2 atmosphere. The measured characteristic Raman frequencies of $C_2O_5^{2-}$ are in excellent agreement with the DFT-model consisting of six overlapping individual theoretical bands calculated from $Li_2C_2O_5$ and $Na_2C_2O_5$.

It is important to point out that the proposed bi-ionic transport model also has implications for rational design of new multicomponent ionic conductor systems for separating and detecting critical gases such as H_2, NO_x, SO_x, Cl_2, Br_2, and F_2, and novel materials containing $(CO_2)_n$ chainlike moieties for high-efficiency large-scale CO_2 uptake and high-density energy storage. New solid-oxide–salt systems will be accordingly explored in the future to uncover new multicomponent heterogeneous ionic conductor systems.

Acknowledgements

This work is supported by the U.S. Army Research Laboratory and the U.S. Army Research Office under grant number W911NF-10-R-006.

References

1 U.S. Energy Information Administration, Energy Perspective 1949–2010, October 19, 2011.
2 U.S. Energy Information Administration, Annual Energy Outlook 2011, April 26, 2011.
3 DOE/NETL, Carbon dioxide capture and storage RD&D roadmap, December 2010.
4 DOE/NETL, Advanced carbon dioxide capture R&D program: technology update, September 2010.
5 L. Zhang, N. Xu, X. Li, S. Wang, K. Huang, W. H. Harris and W. K. S. Chiu, High CO_2 Permeation Flux Enabled by Highly Interconnected Three Dimensional Ionic Channels in Selective CO_2 Separation Membranes, *Energy Environ. Sci.*, 2012, **5**, 8310–8317.
6 R. Bredesen, K. Jordal and O. Bolland, High-temperature membranes in power generation with CO_2 capture, *Chem. Eng. Process.*, 2004, **43**, 1129–1158.
7 B. J. P. Buhre, L. K. Elliott, C. D. Sheng, R. P. Cupta and T. F. Wall, Oxygen-fuel combustion technology for coal-fired power generation, *Prog. Energy Combust. Sci.*, 2005, **31**, 283–307.
8 M. O. Franklin, CO_2 capture and storage: are we ready?, *Energy Environ. Sci.*, 2009, **2**, 449–458.
9 E. Favre, Carbon dioxide recovery from post-combustion processes: can gas permeation membranes compete with absorption?, *J. Membr. Sci.*, 2007, **294**, 50–59.
10 L. Bastin, P. S. Brcia, E. J. Hurtado, J. A. C. Silva, A. E. Rodrigues and B. A. Chen, Microporous metal–organic framework for separation of CO_2/N_2 and CO_2/CH_4 by fixed-bed adsorption, *J. Phys. Chem. C*, 2008, **112**(5), 1575–1581.
11 A. M. Scurto, S. N. V. K. Aki and J. F. Brennecke, CO_2 as a separation switch for ionic liquid–organic mixtures, *J. Am. Chem. Soc.*, 2002, **124**(35), 10276–10277.
12 A. Samanta, A. Zhao, G. K. H. Shimizu, P. Sarkar and R. Gupta, Post-combustion CO_2 capture using solid sorbents: A Review, *Ind. Eng. Chem. Res.*, 2012, **51**(4), 1438–1463.
13 A. B. Rao and E. S. A. Rubin, Technical, Economic, and Environmental Assessment of Amine-Based CO_2 Capture Technology for Power Plant Greenhouse Gas Control, *Environ. Sci. Technol.*, 2002, **36**(20), 4467–4475.
14 H. Kawamura, T. Yamaguchi, N. N. Balagopal, K. Nakagawa and S. Nakao, Dual-Ion Conducting Lithium Zirconate-Based Membranes for High Temperature CO_2 Separation, *J. Chem. Eng. Jpn.*, 2005, **38**(5), 322–328.
15 E. J. Granite and T. O'Brien, Review of novel methods for carbon dioxide separation from flue and fuel gases, *Fuel Process. Technol.*, 2005, **86**, 1423–1434.
16 N. Du, H. B. Park, M. M. Dal-Cin and M. D. Guiver, Advances in high permeability polymeric membrane materials for CO_2 separations, *Energy Environ. Sci.*, 2012, **5**, 7306–7322.
17 J. D. Figueroa, T. Fout, S. Plasynski, H. McIlvried and R. D. Srivastava, Advances in CO_2 capture technology-the US Department of Energy's carbon sequestration program, *Int. J. Greenhouse Gas Control*, 2008, **2**, 9–20.
18 M. A. Carreon, S. Li, J. L. Falconer and R. D. Noble, Alumina-Supported SAPO-34 Membranes for CO_2/CH_4 Separation, *J. Am. Chem. Soc.*, 2008, **130**(16), 5412–5413.
19 M. M. Maroto-Valer, Z. Tang and Y. Zhang, CO_2 capture by activated and impregnated anthracites, *Fuel Process. Technol.*, 2005, **86**(14–15), 1487–1502.
20 C. Stewart and M. A. Hessami, A study of methods of carbon dioxide capture and sequestration—the sustainability of a photosynthetic bioreactor approach, *Energy Convers. Manage.*, 2005, **46**(3), 403–420.
21 ARPA-E Carbon Capture Programs, Taillores Post-Combustion Carbon Capture Workshop, July 11, 2010.
22 C. F. Hendricks, Carbon dioxide removal from coal-fired power plants, *Energy Environ.*, 1994, **1**, 19–49.
23 D. Shekhawal, D. R. Luebke, H. W. Pennline, A review of carbon dioxide selective membranes, National Energy Technology Laboratory, DOE/NETL, 2003.
24 S. Himeno, T. Tomita, K. Suzuki, K. Nakayama, K. Yajima and S. Yoshida, Synthesis and Permeation Properties of a DDR-Type Zeolite Membrane for Separation of CO_2/CH_4 Gaseous Mixtures, *Ind. Eng. Chem. Res.*, 2007, **46**(21), 6989–6997.

25 D. Shekhawat, D. R. Luebke, H. W. A. Pennline, Review of Carbon Dioxide Selective Membranes: A Topical Report. **2003**, DOE/NETL-2003/1200.
26 R. Quinn, J. B. Appleby and P. G. Pez, New facilitated transport membranes for the separation of carbon dioxide from hydrogen and methane, *J. Membr. Sci.*, 1995, **104**(1–2), 139–146.
27 G. Moutiers, M. Gassir and J. Devynck, Oxygen reduced species in molten Li_2CO_3 + K_2CO_3 (42.7 + 57.3 mol%) at 650 °C: a thermodynamic, voltammetric and convolution potential sweep characterization, *J. Electroanal. Chem.*, 1991, **324**, 175–189.
28 A. Borucka, Evidence for the existence of stable $CO_2^{=}$ ion and response time of gas electrodes in molten alkali carbonates, *J. Electrochem. Soc.*, 1977, **124**, 972.
29 J. L. Wade, K. S. Lackner and A. C. West, Transport model for a high temperature, mixed conducting CO_2 separation membrane, *Solid State Ionics*, 2007, **178**, 1530–1540.
30 M. Anderson and Y. S. Lin, Carbonate-ceramic dual-phase membrane for carbon dioxide separation, *J. Membr. Sci.*, 2010, **357**, 122–129.
31 J. L. Wade, C. Lee, A. C. West and K. S. Lackner, Composite electrolyte membranes for high temperature CO_2 separation, *J. Membr. Sci.*, 2011, **369**, 20–29.
32 Z. Rui, M. Anderson, Y. Li and Y. S. Lin, Ionic conducting ceramic and carbonate dual phase membranes for carbonate dioxide separation, *J. Membr. Sci.*, 2012, **417–418**, 174–182.
33 N. Xu, X. Li, M. A. Franks, H. Zhao and K. Huang, Silver-molten carbonate composite as a new high-flux membrane for electrochemical separation of CO_2 from flue gas, *J. Membr. Sci.*, 2012, **401–402**, 190–194.
34 L. Zhang, X. Li, S. Wang, K. G. Romito and K. Huang, High conductivity mixed oxide-ion and carbonate-ion conductors supported by a prefabricated porous solid-oxide matrix, *Electrochem. Commun.*, 2011, **13**, 554–557.
35 L. Zhang, Z. Mao, J. D. Thomason, S. Wang and K. Huang, Synthesis of a homogeneously porous solid oxide matrix with tunable porosity and pore size, *J. Am. Ceram. Soc.*, 2012, **95**, 1832–1837.
36 P. Claes, B. Thirion and J. Gilbert, Solubility of CO_2 in the molten Na_2CO_3–K_2CO_3 (42 mol%) eutectic mixture at 800 °C, *Electrochim. Acta*, 1996, **41**, 141–146.
37 P. Claes, D. Moyaux and D. Peeters, Solubility and salvation of carbon dioxide in the molten $Li_2CO_3/Na_2CO_3/K_2CO_3$ (43.5 : 31.5 : 25.0 mol%) eutectic mixture at 973K. I. Experimental part, *Eur. J. Inorg. Chem.*, 1999, 583–588.
38 P. Claes, D. Moyaux and D. Peeters, Solubility and salvation of carbon dioxide in the molten $Li_2CO_3/Na_2CO_3/K_2CO_3$ (43.5 : 31.5 : 25.0 mol%) eutectic mixture at 973K. II. Theoretical part, *Eur. J. Inorg. Chem.*, 1999, 589–592.
39 K. P. Zeller, P. Schuler and P. Haiss, The Hidden Equilibrium in Aqueous Sodium Carbonate Solutions – Evidence for the Formation of the Dicarbonate Anion, *Eur. J. Inorg. Chem.*, 2005, 168–172.
40 C. Lee, W. Yang and R. G. Parr, *Phys. Rev. B: Condens. Matter Mater. Phys.*, 1988, **37**, 785–789.
41 A. D. Becke, *Phys. Rev. A: At., Mol., Opt. Phys.*, 1988, **38**, 3098.
42 V. A. Rassalov, J. A. Pople, M. Ratner and T. L. Windus, *J. Chem. Phys.*, 1998, **109**, 1223.
43 P. C. Harihan and J. A. Pople, *Theor. Chim. Acta*, 1973, **28**, 213.
44 M. M. Francl, W. J. Pietro, W. J. Hehre, J. S. Binkley, M. S. Gordon, D. J. DeFree and J. A. Pople, *J. Chem. Phys.*, 1982, **77**, 3654.
45 M. J. Frisch, *et al.*, *Gaussian 09, Revision B.01*, Gaussian Inc., Pittsburgh, PA, 2009.
46 T. Helgaker, K. Ruud, K. L. Bak, P. Jørgensen and J. Olsen, *Faraday Discuss.*, 1994, **99**, 165–180.
47 J. B. Bates, M. H. Brooker, A. S. Quist and G. E. Boyd, *J. Phys. Chem*, 1972, **76**, 1565–1571.
48 N. Koura, S. Kohara, K. Takeuchi, S. Takahashi, L. A. Curtiss, M. Grimsditch and M.-L. Saboungi, *J. Mol. Struct.*, 1996, **382**, 163–169.
49 L.-J. Chen, X. Cheng, C.-J. Lin and C.-M. Huang, *Electrochim. Acta*, 2002, **47**, 1475–1480.
50 S. Kohara, N. Koura, Y. Idemoto, S. Takahashi, M.-L. Saboungi and L. A. Curtiss, *J. Phys. Chem. Solids*, 1998, **59**, 1477–1485.
51 R. L. Frost, A. Soisnard, N. Voyer, S. J. Palmer and W. N. Martens, *J. Raman Spectrosc.*, 2009, **40**, 645–649.
52 N. Wen and M. H. Brooker, *J. Phys. Chem.*, 1995, **99**, 359–368.
53 M. E. Boettcher, P.-L. Gehlken, H. Skogby and C. Reutel, *Mineral. Mag.*, 1997, **61**, 249–256.

